0026-895X/07/7103-871–883$20.00
MOLECULAR PHARMACOLOGY
Copyright © 2007 The American Society for Pharmacology and Experimental Therapeutics
Mol Pharmacol 71:871–883, 2007

Vol. 71, No. 3
29686/3181868
Printed in U.S.A.

4-Hydroxy-2-nonenal Adduction of Extracellular Signal-Regulated Kinase (Erk) and the Inhibition of Hepatocyte Erk-Est–Like Protein-1-Activating Protein-1 Signal Transduction

Brante P. Sampey, David L. Carbone, Jonathan A. Doorn, Derek A. Drechsel, and Dennis R. Petersen

Department of Pharmaceutical Sciences, School of Pharmacy, University of Colorado at Denver and Health Sciences Center, Denver, Colorado (B.P.S., D.A.D., D.R.P.); Departments of Pathology and Nutrition, School of Medicine, University of North Carolina at Chapel Hill, Chapel Hill, North Carolina (B.P.S.); Department of Environmental and Radiation Health Sciences, College of Veterinary Medicine and Biomedical Sciences, Colorado State University, Ft. Collins, Colorado (D.L.C.); and Division of Medicinal and Natural Products Chemistry, College of Pharmacy, University of Iowa, Iowa City, Iowa (J.A.D.)

Received August 5, 2006; accepted December 12, 2006

ABSTRACT

4-Hydroxy-2-nonenal (4-HNE) is a major lipid peroxidation (LPO) product formed during oxidative stress. 4-HNE is highly reactive toward cellular nucleophiles and is implicated in the evolution of numerous pathologies associated with oxidative stress and LPO. Recent evidence suggests that chronic pro-oxidant exposure results in the loss of extracellular signal-regulated kinase (Erk)-1/2 phosphorylation in vivo, a signaling pathway associated with cellular proliferation, survival, and homeostasis. Immunodetection and molecular analysis were used in this study to evaluate the hypothesis that 4-HNE modification of Erk-1/2 inhibits constitutive Erk-Est-like protein (Elk)-1-activating protein (AP)-1 signaling. Primary rat hepatocytes treated with subcytotoxic, pathologically relevant concentrations of 4-HNE demonstrated a concentration-dependent loss of constitutive Erk-1/2 phosphorylation, activity, and nuclear localization. These findings were consistent with iron-induced intracellular LPO, which also resulted in a concentration-dependent decrease in hepatocyte Erk-1/2 phosphorylation and activity. 4-HNE and iron-induced inhibition of Erk-1/2 was inversely correlated with the accumulation of 4-HNE-Erk-1/2 monomer adducts. 4-HNE treatment of hepatocytes decreased nuclear total and phosphorylated Erk-1/2, Elk-1, and AP-1 phosphorylation as well as cFos and cJun activities. The cytosolic modification of unphosphorylated Erk-1/2 was evaluated in vitro using molar ratios of inactive Erk-2 to 4-HNE consistent with increasing oxidative stress in vivo. Liquid chromatography combined with tandem mass spectrometry confirmed monomer adduct formation and identified the major adduct species at the histidine 178 residue within the kinase phosphorylation lip. These novel results show that the formation of 4-HNE-Erk-1/2 monomer-adducts results in the inhibition of Erk-Elk-AP-1 signaling in hepatocytes and implicates the His 178 residue with the mechanism of inhibition.

Oxidative stress and the subsequent formation of reactive oxygen species (ROS) have been correlated with a number of disease states, in animal models and in the clinical setting. Recent evidence suggests that the major lipid peroxidation product 4-hydroxy-2-nonenal (4-HNE) is associated with several hepatic disease states, including alcoholic liver disease, hepatic iron overload, hepatitis C, and primary biliary cirrhosis (Paradis et al., 1997a,b). Although the temporal relationship between 4-HNE and oxidative stress has long since been established, the protein-specific effects of pro-oxidant-induced 4-HNE production on hepatic dysfunction have only recently begun to be revealed.

The diverse cellular effects of lipid aldehydes result from their diffusible nature and rapid reactivity (Benedetti et al., 1979). 4-HNE has been shown to modify cysteine (Cys), his-

This work was supported in part by National Institutes of Health/National Institute on Alcohol Abuse and Alcoholism grant R01-AA09300 (to D.R.P.).
Article, publication date, and citation information can be found at http://molpharm.aspetjournals.org.
doi:10.1124/mol.106.029686.

ABBREVIATIONS: 4-HNE, 4-hydroxy-2-nonenal; Erk, extracellular signal-regulated kinase; AP, activating protein; Elk, Est-like protein; LPO, lipid peroxidation; LC, liquid chromatography; MS.MS, tandem mass spectrometry; ECM, extracellular matrix; FeAsc, iron ascorbate; LDH, lactate dehydrogenase; PBS, phosphate-buffered saline; PAGE, polyacrylamide gel electrophoresis; IP, immunoprecipitate(ed); TRE, 12-*O*-tetradecanoylphorbol-13-acetate-responsive element; TPA, 12-*O*-tetradecanoylphorbol-13-acetate; aa, amino acids.

tidine (His), and lysine (Lys) residues via Michael addition, and for Lys, Schiff base products (Esterbauer et al., 1991; Doorn and Petersen, 2002). 4-HNE is known to induce concentration-dependent effects, in that it is cytotoxic to several cell types at high levels (Schaur et al., 1990), promotes both proliferation and apoptosis, and activates some kinases but inhibits others in an apparent cell-dependent manner (Parola et al., 1998; Bae et al., 2000; Ji et al., 2001; Watanabe et al., 2001). Recent evidence demonstrates that in vivo exposure to the pro-oxidant ethanol results in covalent modification of several hepatic enzymes by 4-HNE, including heat shock protein 72, heat shock protein 90, protein disulfide isomerase, and alcohol dehydrogenase (Carbone et al., 2004a,b, 2005a,b). These reports confirm the adduction of hepatic proteins is associated with inhibition of the respective protein function or an increase in their proteasomal degradation. It is also clear from these investigations that chronic oxidant exposure leads to a profound increase in the number of 4-HNE-modified proteins; however, the specific protein targets of 4-HNE modification remain largely unknown.

Recently published data suggest that chronic pro-oxidant exposure decreases the hepatic phosphorylation state of the extracellular signal-regulated kinases (Erk)-1/2 in vivo (Chen et al., 1998; Aroor and Shukla, 2004). In support of this observation, investigations into the neurological and vascular manifestations of chronic alcohol treatment have also revealed an ethanol-mediated loss of normal Erk-1/2 phosphorylation in vivo and in primary culture (Hendrickson et al., 1998; Davis et al., 1999; Chandler and Sutton, 2005). In addition, previous studies have shown that chronic ethanol administration results in the inhibition of normal liver regeneration after partial hepatectomy and chemical liver damage (Wands et al., 1979; Duguay et al., 1982). Knowing that the Erk-1/2 signaling pathway is associated with cell proliferation and survival (Cobb et al., 1994; Chen et al., 2001), the association between pro-oxidant-induced growth inhibition and the inhibition of this pathway becomes clear. Although some investigations suggest that 4-HNE activates Erk-1/2 phosphorylation in cultures of various cell lines (Iles et al., 2003; Iles and Liu, 2005), recent evidence shows that cell lines profoundly differ from their primary counterparts with respect to 4-HNE metabolism and sensitivity (Canuto et al., 1993, 1994). These observations emphasize the justification for using primary cells when investigating the effects of 4-HNE on normal, constitutive cellular functions in particular signal transduction pathways.

The extracellular signal-regulated kinases-1/2 are members of the mitogen-activated protein kinase family that are redundant, highly homologous (>83% identical) signal transduction intermediates collectively referred to as Erk-1/2 (Chen et al., 2001). The Erk-1/2 pathway is associated with cellular proliferation, survival, differentiation, and homeostasis (Cobb et al., 1994; Chen et al., 2001). The proliferative, prosurvival, and homeostatic roles of Erk-1/2 signaling are mediated through the substrate Elk-1 to the transcription factor AP-1, resulting in the transcription of functionally related genes (Pearson et al., 2001). From a mechanistic standpoint, activation of Erk-1/2 occurs through its phosphorylation via the mitogen-activated protein kinase kinase-1/2, dimerization, and active nuclear translocation, resulting in the phosphorylation and activation of Elk-1, and subsequently AP-1 (Cobb et al., 1994; Chen et al., 2001; Pearson et al., 2001). Erk-mediated activation of AP-1 preferentially occurs with the cFos isoform and to a lesser extent cJun (Cobb et al., 1994). Therefore, LPO-mediated inhibition of constitutive Erk-1/2 phosphorylation in the liver potentially results in the loss of signal transduction and transcriptional activity affecting hepatic homeostasis, proliferation, and survival.

Although ethanol-induced oxidative stress has been implicated in the loss of Erk-1/2 phosphorylation (Davis et al., 1999; Aroor and Shukla, 2004; Chandler and Sutton, 2005) and the accumulation of 4-HNE-protein adducts (Sampey et al., 2003; Carbone et al., 2004a, 2005a), the mechanistic association between these two events remains unresolved. In the present study, we sought to determine the effects of 4-HNE on the constitutive activity of Erk-1/2 in primary hepatocytes by using concentrations of 4-HNE consistent with those observed in vivo. Parallel studies were also conducted using iron ascorbate to evaluate the effects of intracellular LPO on hepatocyte Erk-1/2. In addition, liquid chromatography, tandem mass spectrometry (LC-MS/MS) analysis of 4-HNE-modified Erk-2 was used to elucidate the mechanism of inhibition observed in primary culture. The results of these experiments show that 4-HNE and iron ascorbate result in the concentration-dependent inhibition of constitutive Erk-1/2 phosphorylation and activity. In addition, treatment of hepatocytes with 4-HNE leads to a similar decrease in both total and phosphorylated nuclear Erk-1/2, resulting in loss of Elk-1 phosphorylation, and loss of nuclear cFos and cJun activity. LC-MS/MS verified adduction of inactive Erk-2 monomers, suggesting the involvement of the His 178 adduct within the activation loop of Erk-2 in the 4-HNE-mediated mechanism of kinase inhibition observed in hepatocytes.

Materials and Methods

Materials. All chemicals and reagents used were of the highest purity and obtained from Sigma-Aldrich (St. Louis, MO) unless otherwise indicated. 4-HNE was synthesized just before use as described by Mitchell and Petersen (1991). Purified, unphosphorylated mouse Erk-2, monoclonal and polyclonal antibodies against total and phospho-specific Erk-1/2, Elk-1, and pan-AP-1, and components for nonradioactive detection of kinase activity were obtained from Cell Signaling Technology Inc. (Beverly, MA). Polyclonal antibodies against (rat) GST-Ya were purchased from Oxford Biomedical Research (Oxford, MI). Sequencing grade trypsin was obtained from Promega (Madison, WI). Polyclonal antibodies against 4-HNE-protein adducts recognizing Cys, His, and Lys adducts were developed by our laboratory as described previously (Hartley et al., 1997). Cell culture media, penicillin/streptomycin, and fetal bovine serum were obtained from Mediatech (Herndon, VA).

Sequence Analysis. The amino acid sequences for the extracellular signal-regulated kinase 1 from *Mus musculus*, *Rattus norvegicus*, and *Homo sapiens* were obtained from National Center for Biotechnology Information (NP036082, NP059043, and NP002737, respectively), and the extracellular signal-regulated kinase 2 (or *Xenopus laevis* equivalent, myelin basic protein kinase) from *M. musculus*, *R. norvegicus*, *X. laevis*, and *H. sapiens* were obtained from National Center for Biotechnology Information (P63085, P63086, P26696, and P28482, respectively). These sequences were manually aligned according to the human sequence to determine the extent of homology and conservation of potential 4-HNE-reactive sites between the Erk isoforms and across experimental species, compared with the human Erk-1/2 sequence.

Primary Rat Hepatocyte Isolation and Culture Conditions. All animal procedures were approved by the University of Colorado Health Sciences Center Institutional Animal Care and Use Committee and were conducted in accordance with published National Institutes of Health guidelines. Primary rat hepatocytes were isolated from naive, laboratory chow-fed male Sprague-Dawley rats (>400 g) purchased from Harlan (Indianapolis, IN) using a modification of the collagenase perfusion method and differential centrifugation as described previously (Hartley and Petersen, 1997; Hartley et al., 1997). Isolated hepatocytes were resuspended in RPMI 1640 medium containing penicillin/streptomycin (100 IU/ml and 100 μg/ml, respectively), and the cells were seeded onto 100-mm tissue culture plates (BD Biosciences, Franklin Lakes, NJ) coated with extracellular matrix (ECM) at a concentration of 3.5 million cells/plate. Adherent hepatocytes were allowed to acclimate to culture conditions at 37°C, 5% CO_2 overnight before treatment with aldehyde or iron ascorbate. Viability of isolated cells was determined by trypan blue exclusion and adherence to ECM-coated plates.

Primary Hepatocyte Treatment. Primary rat hepatocyte cultures were used to determine the effects of 4-HNE and the prooxidant iron ascorbate (FeAsc) on the constitutive Erk-1/2 signaling pathway. After an overnight acclimation period, media were removed from primary hepatocytes and replaced with serum-free RPMI 1640 medium containing 0, 0.01, 0.1, 1.0, 10, and 100 μM 4-HNE or 0, 0.188, 0.375, 0.750, and 1.500 mM FeAsc for 4 h under normal cell culture conditions, a time previously shown to be effective in similar experiments (Tjalkens et al., 1998). At the end of treatment, media and an aliquot of cells were collected for cytotoxicity assessment before evaluation of cells for total and nuclear protein isolation.

Biochemical Assays. 4-HNE cytotoxicity was determined using the in vitro cytotoxicity assay (Tox-7; Sigma-Aldrich) according to the manufacturer's protocol. Cytotoxicity was indirectly quantified as the ratio of lactate dehydrogenase (LDH) activity in the media (released) over the total cellular LDH activity. Media and an aliquot of cells were collected at the appropriate times for each cell treatment group and used immediately to determine LDH activity. Control media and phosphate-buffered saline (PBS) with protease inhibitors served as negative controls. LDH conversion of NAD to NADH was measured using a Spectra Max 190 (Molecular Devices, Sunnyvale, CA) plate reader, and the data were collected using SoftMax Pro 4.0 (Molecular Devices). Relative cytotoxicity is reported as the ratio of absorbance corresponding to released LDH activity over the total cellular LDH activity, compared with untreated control cells.

In addition, FeAsc-induced intracellular lipid peroxidation was confirmed using the LPO assay kit (OXIS International Inc., Foster City, CA), as per the manufacturer's protocol. Lipid peroxidation is presented as the concentration of hydroxyalkenals + malondialdehyde per milligram of protein for each treatment group.

Cell Harvest and Protein Isolations. At the end of each treatment, the primary hepatocytes were liberated from the ECM-coated plates with ice-cold PBS/1 mM EDTA solution using a cell lifter, and the cells were centrifuged at 500*g* before being resuspended in PBS containing 4 μl/ml protease inhibitor cocktail. Total cell extracts were prepared by sonicating the hepatocyte suspensions four times each, for 5 s on ice using a Sonic Dismembrator model 100 (Fisher Scientific, Pittsburgh, PA), centrifuged to remove cellular debris from the protein fraction, and the total cell extract protein was quantified using a BCA protein assay kit (Pierce Chemical, Rockford, IL). Proteins were diluted to 1 mg/ml and either used immediately for kinase activity assays or mixed with 6× SDS-PAGE loading buffer, heated to 100°C for 5 min, and separated using SDS-PAGE for immunoblot analysis. Alternatively, nuclear protein fractions were isolated from cell treatment groups using a nuclear isolation kit (Active Motif, Inc., Carlsbad, CA) as per the manufacturer's protocol. Nuclear protein fractions were quantified and diluted in PBS to a final concentration of 1 mg/ml.

SDS-PAGE Separation and Immunoblot Analysis. Total cell extract, immunoprecipitated protein, or recombinant protein was separated using SDS-PAGE made up of a 4% stacking and a 12% resolving gel for 2 h at 50 mA in a Bio-Rad mini-gel system (Bio-Rad, Hercules, CA). Proteins transferred to polyvinylidene difluoride membranes using a semidry transfer apparatus (Bio-Rad), were blocked in 5% (w/v) bovine serum albumin in Tris-buffered saline-Tween 20 at room temperature for 45 min. Primary antibodies against total and phospho-specific Erk-1/2, phospho-specific Elk-1, and phospho-specific pan-AP-1 were diluted according to the manufacturer's recommendation in 5% bovine serum albumin/Tris-buffered saline-Tween 20 and allowed to incubate overnight at 4°C. They were then washed, and the horseradish peroxidase-linked secondary antibodies were used to detect primary antibodies via incubation for 45 min at room temperature. Membranes were washed and treated with ECL-Plus (GE Healthcare, Little Chalfont, Buckinghamshire, UK) enhanced chemiluminescence reagent. Antibody-reactive protein bands were visualized using film and a GE Healthcare STORM 860 PhosphorImager and quantified using ImageQuant version 5.2 software (GE Healthcare). For total cell extracts, immunoblots were stripped and reprobed for β-actin to demonstrate equal loading. For nuclear extracts, gels were stained with Coomassie Blue to demonstrate equal loading.

Erk-1/2 Activity Assay. To determine whether 4-HNE and/or FeAsc affects constitutive Erk-1/2 activity toward its substrate Elk-1, a nonradioactive kinase assay was used as described previously (Tyagi et al., 2003). Monoclonal antibodies raised against phospho-Erk-1/2 conjugated to agarose beads were used to immunoprecipitate (IP) Erk-1/2 from 250 μg of total cell lysates. The immunoprecipitated proteins were washed free of other proteins and incubated with an Elk-1 fusion protein (2 μg/reaction) in the presence of 200 μM ATP for 30 min at 37°C. The reactions were stopped by addition of 6× SDS/PAGE loading buffer, incubated at 100°C for 5 min, vortexed, and centrifuged at room temperature. Immunoblot using polyclonal antibodies specific for phospho-Elk-1 were used to determine the ability of IP-Erk-1/2 to phosphorylate an Ekl-1 fusion protein. 4-HNE-Erk-1/2 adducts were determined using identical blots probed with antibodies raised against 4-HNE-protein adducts. Immunoblots were visualized and quantified as described above.

Identification of Active Nuclear AP-1 Subunits. The effect of 4-HNE on the constitutive activity of Erk-1/2-responsive AP-1 subunits, namely, cFos and cJun, were determined using nuclear extracts from primary cultures treated with aldehyde at 0, 1, and 100 μM as determined by the Active Motif TransAM method. In brief, 15 μg of nuclear extract from control or aldehyde-treated hepatocyte cultures were incubated in separate wells of a 96-well plate possessing an immobilized AP-1 consensus sequence [TPA-responsive element (TRE) oligonucleotide 5′-TGAGTCA-3′], inactive AP-1 molecules were removed with wash buffer, and the active TRE-bound AP-1 was identified using primary antibodies directed against the cFos and cJun subunits in conjunction with horseradish peroxidase-conjugated secondary antibodies and a colorimetric substrate quantified by spectrophotometry.

In Vitro Modification of Erk-2 by 4-HNE and Tryptic Digest. Mouse recombinant Erk-2 (250 ng; 0.2 μM) was incubated in the presence of 0, 0.01, 0.10, 1.00, 10.0, or 100 μM 4-HNE in 50 mM sodium phosphate buffer, pH 7.4, for 4 h at 37°C, corresponding to 4-HNE:Erk-2 molar ratios of 0.05:1, 0.5:1, 5:1, 50:1, and 500:1, respectively; ratios calculated to mimic in vivo conditions of oxidative stress according to the literature (Benedetti et al., 1980; Esterbauer et al., 1991). For immunoblot analysis, the reaction was stopped by the addition of 6× SDS-PAGE loading buffer, mixed thoroughly, and incubated at 100°C for 5 min. For mass spectral analysis, the reaction was stopped by the addition of 2 mM β-mercaptoethanol, and the protein was thermally denatured at 90°C for 5 min. The denatured protein was then cooled to room temperature, and upon the addition of 10% acetonitrile and trypsin (20:1 protein/trypsin ratio), digested for 4 h at 37°C.

Mass Spectral Analysis. Mass spectral analysis of native or 4-HNE-modified Erk-2 was carried out as described previously (Carbone et al., 2004a). In brief, tryptic digests (8 μl) from pure, recombinant Erk-2 or Erk-2 treated with 4-HNE were evaluated by LC-MS/MS analysis of peptides using an Agilent Technologies (Palo Alto, CA) 1100 series LC/electrospray ionization–mass-selective detector trap equipped with a Phenomenex (Torrance, CA) Jupiter C18 column (1 × 150 mm; 300 Å). The mobile phase consisted of 0.2% formic acid in water (A) and 0.2% formic acid in acetonitrile (B) with flow rate of 50 μl/min and gradient conditions as follows: 5% B at 0 min, 5% B at 5 min, 70% B at 35 min, 90% B at 38 min and held for 2 min, and 5% B at 42 min and held for 3 min. Mass spectrometric detection and analysis was accomplished using positive ion mode with a capillary voltage of 3.5 kV. Nebulizer pressure was set at 20 psi, and dry gas flow was set at 8 l/min with the temperature of the dry gas set to 350°C. The scanning range for all analyses was 400 to 2000 m/z and peptides within the mass range of 500 to 1500 Da were subject to MS/MS analysis. MS/MS ion search was performed on deconvoluted spectra using MASCOT. Tryptic peptides were calculated using the MS-Digest feature of Protein Prospector version 4.0.5 (http://prospector.ucsf.edu). Peptides modified by 4-HNE were identified on the basis of the presence of the parent peptide in both treated and untreated protein digests, in addition to a mass shift of the parent peptide equal to that of 4-HNE (156 Da) in the treated protein. The presence of a 4-HNE adduct and the site of modification were confirmed and mapped, respectively, via MS/MS analysis. Predicted fragment ions were calculated using the MS-Product feature of Protein Prospector version 4.0.5 (Mass Spectrometry Facility, University of California, San Francisco, CA).

Statistical Analysis. The numerical data associated with each immunoblot are presented as mean density units normalized to that of control, which was given a value of 1. Comparisons between constitutive control values and 4-HNE-treatment values or FeAsc-treatment values are expressed as -fold control. Representative blots and data corresponding to highly reproducible, independent experiments are shown as the mean ± S.E.M. ($n \geq 3$). Where applicable, statistically significant differences between control and 4-HNE-treated groups or between control and FeAsc-treated groups were determined using the Student's t test (SigmaPlot 6.0; SPSS Inc., Chicago, IL). Mean values were declared significantly different at $p < 0.05$, although in certain cases the level of significance was much greater.

Results

The amino acid sequences were compared between Erk-1 and Erk-2 from *M. musculus*, *R. norvegicus*, and *H. sapiens*, and among the homologs of Erk-2 (or the Erk-2 homolog myelin basic protein kinase kinase) from *H. sapiens*, *M. musculus*, *R. norvegicus*, and *X. laevis*, which were manually aligned revealing a highly conserved core region between the isoforms (>83% identical) and across the species, which were all >96% identical to human. Because 4-HNE preferentially modifies Cys, His, and Lys residues, these sequences were evaluated to determine the number of potential sites of adduction for each species of Erk-2, which were all conserved in experimental variants compared with those found in the human sequence, as well as being conserved between the Erk-1 and Erk-2 isoforms of the rat. These results support the use of experimental variants of Erk-1/2 as appropriate alternatives to the human form, with the mouse and rat Erk-2 amino acid sequences used in the experiments herein varying from human by less than 1%.

Characterization of 4-HNE and FeAsc Cytotoxicity. Primary rat hepatocyte cultures were exposed to a range of concentrations of 4-HNE and FeAsc to identify a cytotoxic threshold for each agent (Fig. 1A). Cytotoxicity associated with cells treated with increasing concentrations of 4-HNE demonstrates that, compared with 4-h controls (no cytotoxicity), 4-HNE concentrations ranging from 0.01 to 100 μM did not result in significant cytotoxicity. However, when exposed to 1000 μM 4-HNE, a dramatic increase in released/cellular LDH activity ratio occurred (>20-fold over control; $p < 0.0001$), reflective of marked cytotoxicity. Given these results, subcytotoxic concentrations of 4-HNE (0.01–100 μM) were used for the experiments reported here. In addition, a range of FeAsc concentrations was evaluated to determine its cytotoxicity toward primary hepatocytes in culture. Figure 1B shows that concentrations of 0.188 and 0.375 mM FeAsc had no significant cytotoxic effects compared with control. At 0.750 and

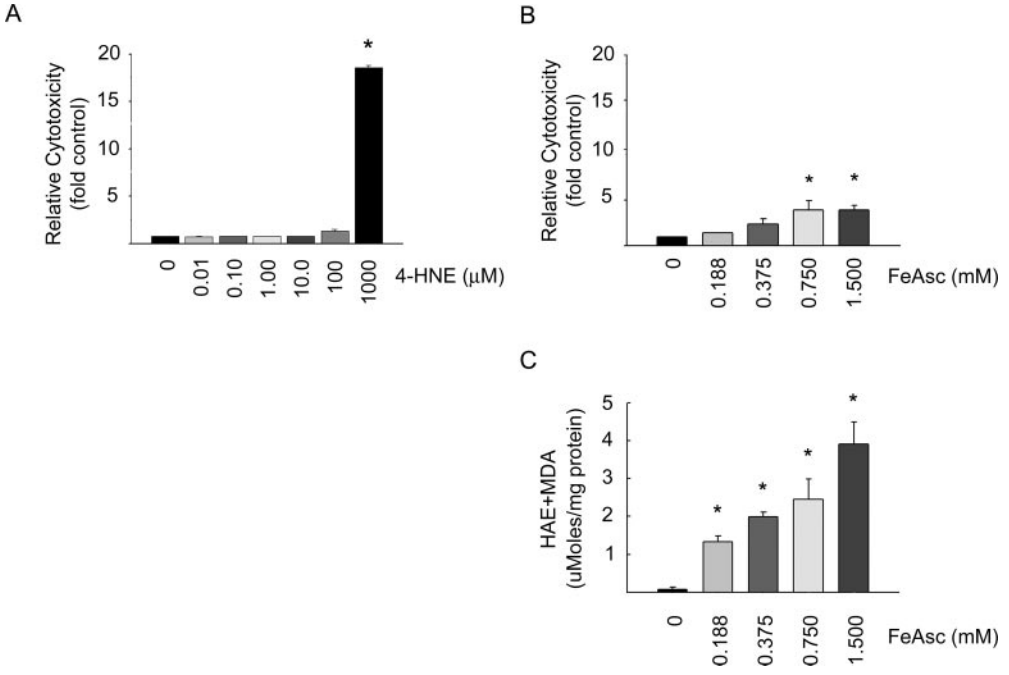

Fig. 1. A, physiologically relevant concentrations of 4-HNE were tested to determine the subcytotoxic concentration range to be used for subsequent experiments after 4-h treatments. Values represent the ratio of LDH activity released into the media of primary hepatocyte cultures over the total cellular LDH activity, when normalized to untreated controls. B, cytotoxicity of the pro-oxidant FeAsc was evaluated over a range of concentrations using the LDH ratio method described previously. C, FeAsc-induced lipid peroxidation in primary hepatocytes was quantified as described under *Materials and Methods* over a range of concentrations. All values presented represent mean ± S.E.M. for $n = 4$ independent experiments. Asterisks indicate a significant difference $p \leq 0.05$ compared with 0.00 μM 4-HNE treatment (vehicle control).

1.500 mM concentrations, FeAsc exposure increased cytotoxicity that reached statistical significance ($p < 0.05$). It is important to note that the increased cytotoxicity associated with these latter two concentrations of FeAsc was associated with significant increases in loss of membrane integrity (released LDH activity), but not with loss of total cell numbers (total cellular LDH activity). Thus, these cellular responses to this pro-oxidant stimuli are <5-fold below the prominent cytotoxicity demonstrated by 1000 μM 4-HNE. These observations are consistent with the data presented in Fig. 1C showing a concentration-dependent increase in lipid peroxidation, as determined by the increase in lipid aldehyde concentrations. Based on a comparison of relative cytotoxicity profiles between 4-HNE and FeAsc, (Fig. 1, A and B, respectively), intracellular concentrations of 4-HNE that result from treatment of hepatocytes with 0.188 mM FeAsc are equivalent to exogenous treatment with 100 μM 4-HNE, and the subsequent increasing concentrations of FeAsc would fall within the lower end of the 100 to 1000 μM aldehyde treatment range, as determined by the lack of robust toxic effects with 1.500 mM FeAsc, which was seen with 1000 μM 4-HNE. Therefore, this concentration range of FeAsc (0.188–1.500 mM) was maintained throughout the remainder of the studies reported here.

Subcytotoxic Concentrations of 4-HNE and FeAsc Modulate Constitutive Erk-1/2 Phosphorylation and Activity. To evaluate whether 4-HNE and/or FeAsc modulates hepatic Erk signaling, primary rat hepatocyte cultures were exposed to subcytotoxic concentrations of 4-HNE or FeAsc over a 4-h period (Tjalkens et al., 1998). Figure 2A shows a representative immunoblot and corresponding densitometry analysis for total Erk-1/2 using total cell extracts from primary hepatocytes treated with 0.00 to 100.0 μM 4-HNE. These data show that over a broad concentration range, 4-HNE does not affect total Erk-1/2 protein levels in primary hepatocytes. Likewise, as shown in Fig. 2B, cells exposed to a range of FeAsc concentrations that result in increasing lipid peroxidation also lack changes in total Erk-1/2 concentrations in total cell extracts. However, the data in Fig. 2C clearly show that Erk-1/2 phosphorylation significantly decreases in a concentration-dependent manner when hepatocytes are challenged with levels of 4-HNE (0.10–100 μM). Likewise, FeAsc treatment (0.188–1.500 mM) of hepatocytes resulted in a decrease in phospho-Erk-1/2 concentrations that was also concentration-dependent (Fig. 2D).

A nonradioactive kinase activity assay was used to determine whether the results shown in Fig. 2, C and D, correlated with Erk-1/2 activity toward its substrate Elk-1. Erk-1/2 was immunoprecipitated from the total cell extracts of hepato-

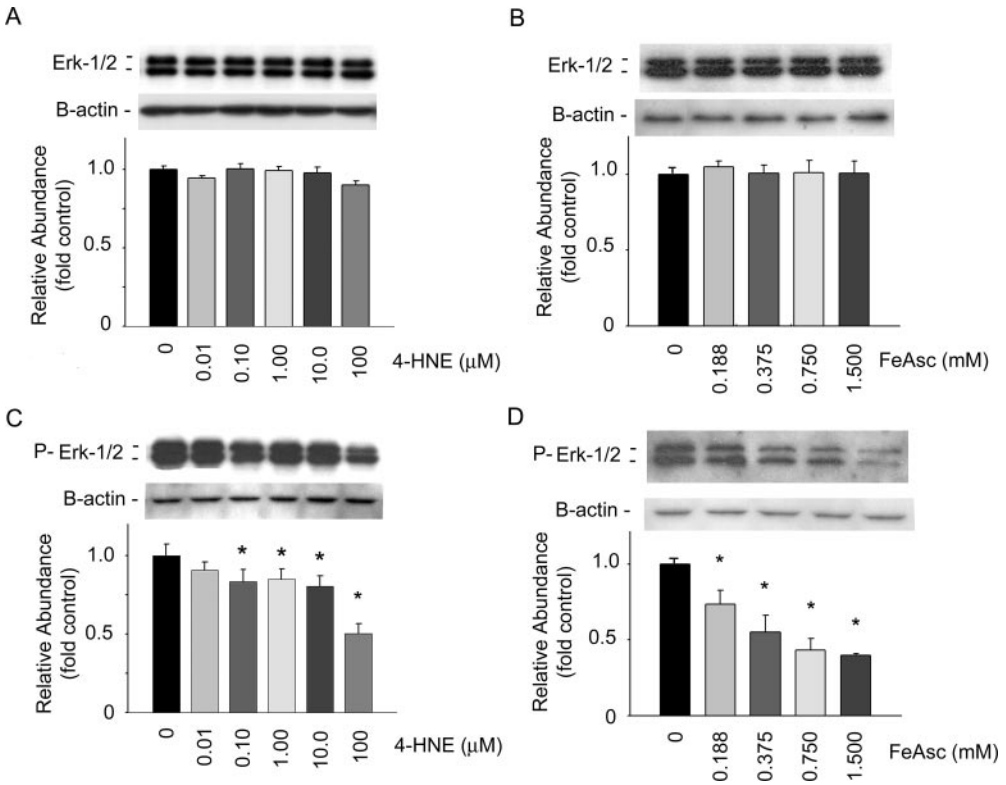

Fig. 2. Subcytotoxic concentrations of 4-HNE and FeAsc were used to evaluate their effects on Erk-1/2 in primary hepatocyte cultures after 4-h exposure. A, 4-h exposure to the indicated concentrations of 4-HNE had no effect on total Erk-1/2 concentrations in total hepatocyte extracts, as determined by immunoblot and corresponding densitometry analysis. Values represent mean ± S.E.M. for $n = 9$ measurements. B, 4-h exposure to concentrations of FeAsc shown to produce increasing lipid peroxidation in primary hepatocytes demonstrated no effect on total Erk-1/2 concentrations in total cell extracts, as determined by immunoblot and corresponding densitometry analysis. Values represent mean ± S.E.M. for $n = 4$ independent experiments. C, 4-h exposure to the indicated concentrations of 4-HNE resulted in a concentration-dependent decrease in phosphorylated Erk-1/2 concentrations in total hepatocyte extracts, as determined by immunoblot and corresponding densitometry analysis. Asterisks indicate a significant difference ($p \leq 0.05$) compared with 0.00 μM 4-HNE treatment (vehicle control) for the number of determinations indicated in A. D, 4-h exposure to increasing concentrations of FeAsc resulted in a concentration-dependent decrease in phosphorylated Erk-1/2 levels in total hepatocyte extracts, as determined by immunoblot and corresponding densitometry analysis. Asterisks indicate a significant difference ($p \leq 0.05$) compared with 0.00 mM FeAsc treatment (control) for $n = 4$ measurements. β-actin controls are shown in each figure to demonstrate equal protein loading across each sample group.

cytes using the conditions described above and incubated with substrate (Elk-1) and ATP, and the components of these reactions were separated using SDS-PAGE and probed for the substrate phosphorylated Elk-1. The immunoblot and corresponding densitometry in Fig. 3A show that 4-HNE results in a pattern of significant concentration-dependent decrease in Elk-1 phosphorylation that is consistent with the 4-HNE-mediated decrease in Erk-1/2 phosphorylation (Fig. 2C). The inset in Fig. 3A confirms that concentrations of 4-HNE from 0.01 to 100 μM fail to inhibit the activity of IP-phospho-Erk-1/2 from control cells indicating 4-HNE-mediated inhibition of Erk-1/2 activity results from aldehyde modification of the inactive, unphosphorylated monomers. The FeAsc-mediated decrease in Erk-1/2 phosphorylation shown in Fig. 2D resulted in a concentration-dependent decrease in Erk-1/2 activity similar to that after 4-HNE treatment, as shown in Fig. 3B. Data in Fig. 3, C and D, show that in primary hepatocytes the decrease in Erk-1/2 activity resulting from increased 4-HNE treatment and FeAsc treatment, respectively, is inversely correlated with the level of 4-HNE-Erk-1/2 adduct concentration. It is important to note that the bands representing 4-HNE-modified Erk-1/2 correspond to the molecular mass of Erk monomers (41 and 43 kDa). The data presented in Figs. 2 and 3 show collectively that exogenous and endogenous 4-HNE results in aldehyde-Erk monomer adducts that occur concurrent with inhibition of constitutive Erk-1/2 phosphorylation and activity as reflected in decreased phosphorylation of its substrate Elk-1.

4-HNE Attenuates Nuclear Erk-Elk-AP-1 Signal Transduction. The activation of Erk-1/2 has been shown to affect transcriptional and translational activities; however, the nuclear localization of Erk-1/2 is a prerequisite for survival and proliferation through the AP-1 transcription factors (Cobb et al., 1994; Karin, 1995; Tyagi et al., 2003). Although the 4-HNE responses described above established aldehyde-mediated modulation of constitutive Erk-1/2, it was important to determine whether these results yield a correlative modulation of nuclear concentrations of Erk-1/2. Consequently, the 4-HNE effects on Erk-1/2-mediated transcription were explored by comparing the activation states of total cellular and nuclear Erk-1/2 by using cells treated as described above. Nuclear proteins were subjected to SDS-PAGE separation and subsequent immunoblot analysis using antibodies against total or phospho-Erk-1/2. The purity of nuclear proteins was determined by the absence of positive band staining on these nuclear blots when stripped and reprobed with the cytosolic marker GST-Ya (data not shown). Contrary to the studies using total cell lysates, Fig. 4A shows a representative immunoblot indicating that incubation of hepatocytes with increasing concentrations of 4-HNE leads to a decrease in total nuclear Erk-1/2 concentrations that attained significance at 4-HNE concentrations of 1.0 μM. Not

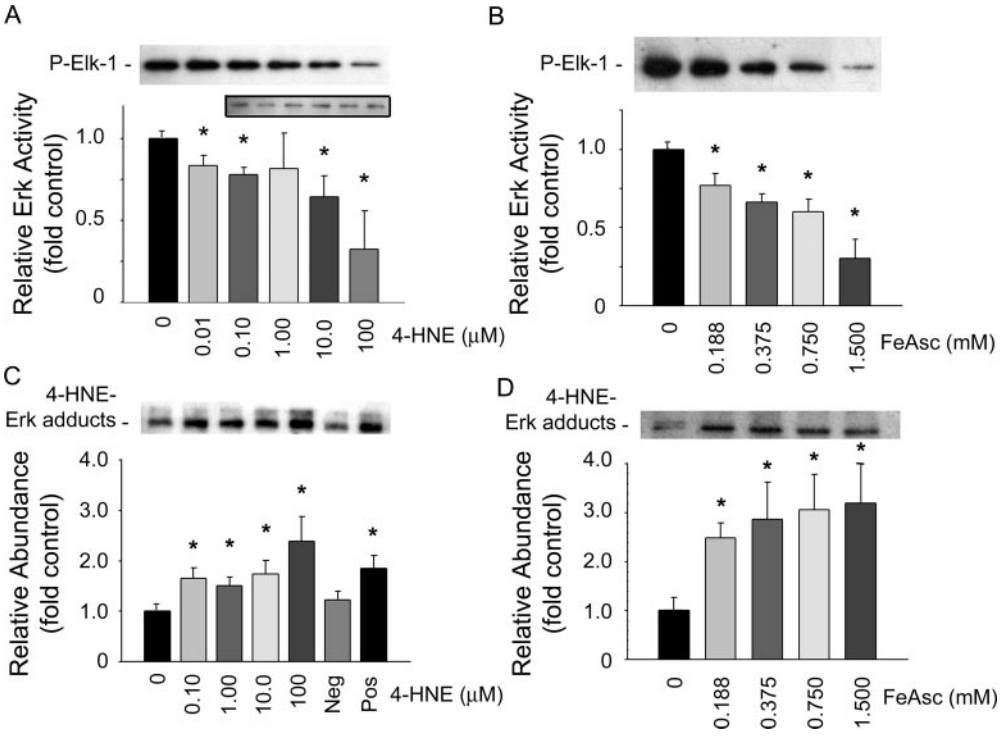

Fig. 3. 4-HNE and FeAsc were evaluated for their ability to inhibit Erk-1/2 activity through covalent modification of Erk molecules. A, increasing concentrations of 4-HNE inhibited constitutive Erk-1/2 activity after 4-h exposure in a concentration-dependent manner. Values represent mean ± S.E.M. for $n = 5$ measurements. Asterisks indicate a significant difference ($p \leq 0.05$) compared with 0.00 μM 4-HNE treatment. A, inset, immunoblot associated with Erk-1/2 kinase assay demonstrating the activity of phosphorylated Erk-1/2 IP from control hepatocytes is unaffected by subsequent treatment with increasing concentrations of 4-HNE. B, increasing concentrations of FeAsc inhibited constitutive Erk-1/2 activity in primary hepatocytes after 4-h exposure in a concentration-dependent manner, as determined by kinase activity assay described under *Materials and Methods*. Asterisks indicate a significant difference ($p \leq 0.05$) compared with 0.00 mM FeAsc treatment. C, concentrations of 4-HNE ranging from 0.10 to 100 μM increased the levels of 4-HNE-Erk monomer adducts in cell extracts after cells were exposed to aldehyde for 4 h, as shown by immunoblot and densitometry analysis of IP-Erk-1/2 when probed for 4-HNE-protein adducts (described under *Materials and Methods*). D, increasing concentrations of FeAsc significantly increased the levels of 4-HNE-Erk monomer adducts in cell extracts when cells were exposed to pro-oxidant for 4 h. All data are presented as mean ± S.E.M. for $n = 3$ to 5 individual experiments. *, $p \leq 0.05$ compared with the respective controls.

surprisingly, 4-HNE was also shown to significantly decrease the nuclear phosphorylated Erk-1/2 concentrations over the entire range of 4-HNE concentrations (Fig. 4B). Because activation of Erk-1/2 is required for nuclear localization (Chen et al., 2001; Pearson et al., 2001), these data suggest that adduction and inhibition by 4-HNE occurs with the inactive monomer in the cytosolic compartment.

Having established that 4-HNE resulted in a loss of Erk-1/2 activity in total cell extracts (Fig. 3A), nuclear extracts from aldehyde-treated cells were analyzed to confirm a concentration-dependent loss of Erk-1/2 substrate phosphorylation. As shown in Fig. 4C, increasing concentrations of 4-HNE ranging from 0.1 to 100 μM resulted in a significant loss of constitutive Elk-1 phosphorylation. It is apparent in

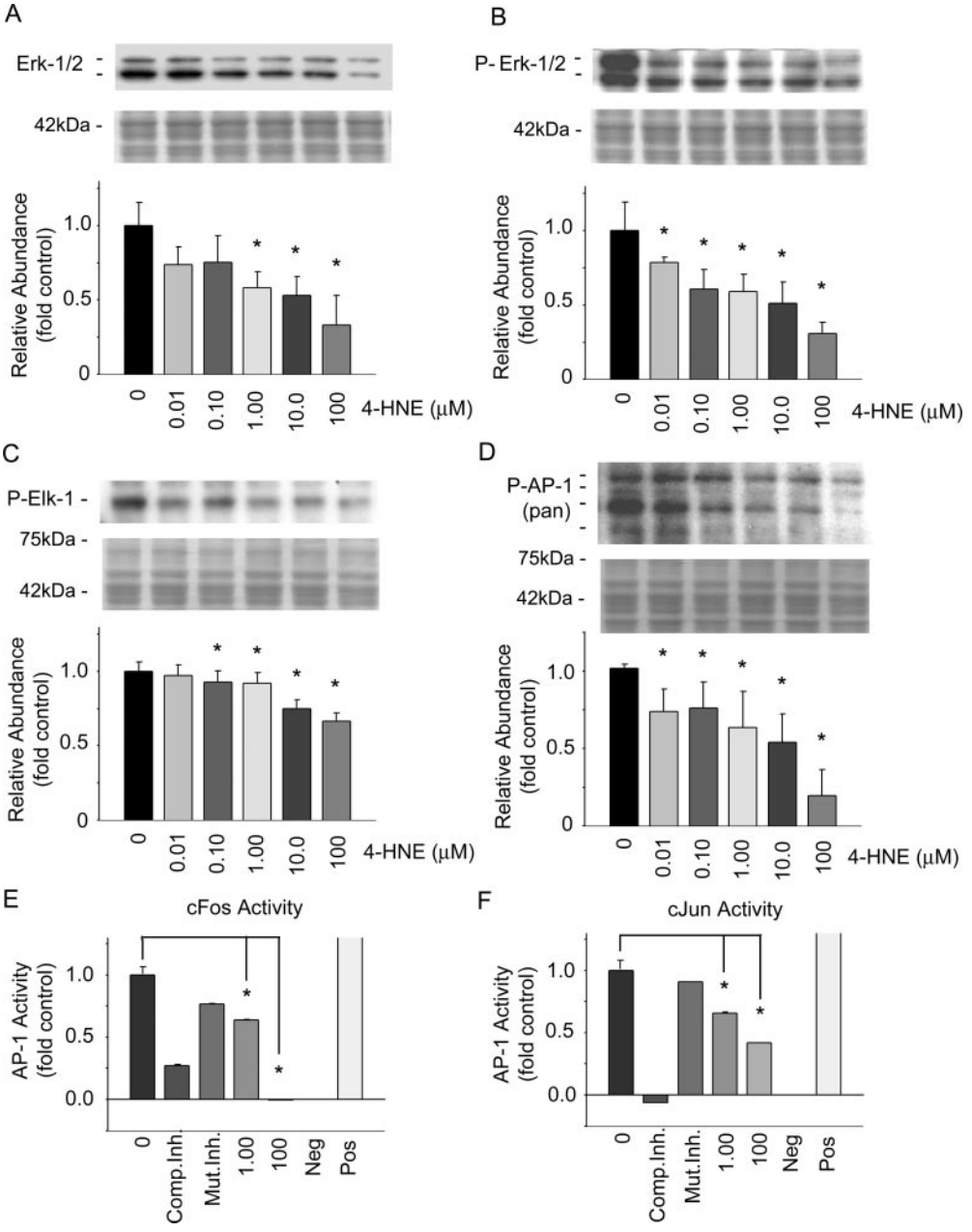

Fig. 4. 4-HNE (4-h treatment) was evaluated for its ability to inhibit Erk-Elk-AP-1 signaling. Increasing concentrations of 4-HNE decreased nuclear concentrations of total Erk-1/2 (A) and phosphorylated Erk-1/2 (B) in a concentration-dependent manner, as determined by immunoblot and densitometry analysis of nuclear protein fractions. Increasing concentrations of 4-HNE decreased nuclear concentrations of phosphorylated Elk-1 (C) and several phosphorylated components of the AP-1 transcription factor (D), as determined by immunoblot and densitometry analysis of nuclear protein fractions. Equal loading of gel lanes was demonstrated using Coomassie Blue stain on gels after transfer and are present beneath each blot in A to D. E, 4-HNE inhibited nuclear cFos activity toward its consensus sequence (TRE), with complete inhibition occurring at 100 μM 4-HNE ($p < 0.001$ for both aldehyde concentrations), as determined by transcription factor activity assay described under *Materials and Methods*. This effect was equivalent to negative control (Neg) and was below the activity level of cFos isolated from control cells when the consensus sequence was first challenged with a competitive inhibitor (Comp.Inh.). F, 4-HNE inhibited nuclear cJun activity toward its consensus sequence, with significant yet incomplete inhibition occurring at 100 μM 4-HNE ($p < 0.001$), as determined by transcription factor activity assay described under *Materials and Methods*. This effect was equivalent to negative control (Neg) and was below the activity level of cJun isolated from control cells when the consensus sequence was first challenged with a competitive inhibitor (Comp.Inh.). Values represent mean ± S.E.M. for $n = 3$ to 4 independent experiments. *, $p \leq 0.05$ compared with the respective control values.

Fig. 4D that the loss on Elk-1 parallels the loss of phosphorylation of several isoforms of AP-1, when nuclear extracts were evaluated using antibodies against phosphorylated pan AP-1. 4-HNE-mediated inhibition of constitutive AP-1 phosphorylation was confirmed via evaluation of nuclear cFos and cJun activity toward the TRE sequence using the nuclear extracts from hepatocytes treated with aldehyde. Data in Fig. 4E demonstrate that 1 and 100 μM 4-HNE treatment of primary hepatocytes results in a significant loss of cFos activity toward its consensus sequence that is completely ablated at the higher concentration (similar to negative control and significantly less than control samples treated with competitive inhibitor). These observations were similar for the cJun isoform of AP-1, although to a lesser degree than for the primary Erk-1/2-modulated AP-1 constituent (cFos). These data show collectively that exogenous 4-HNE inhibits constitutive Erk-Elk-AP-1 signal transduction by preventing Erk-1/2 nuclear localization, resulting in the complete ablation of nuclear cFos activity in primary hepatocytes.

4-HNE Modifies Inactive Erk-2 Monomers. Because the results reported above suggest an inhibitory mechanism mediated by the adduction of inactive cytosolic Erk monomers, the effects of 4-HNE on unphosphorylated Erk monomers were investigated. Inactive recombinant Erk-2 was incubated with vehicle and concentrations of 4-HNE ranging from 0.01 to 100 μM to evaluate the ability of 4-HNE to modify Erk-2 monomers. Such conditions simulate molar ratios present during mild to marked oxidative stress (Esterbauer et al., 1991; Chen et al., 2001) and are the same as those established in primary cultures reported above. Figure 5A is a representative immunoblot demonstrating 4-HNE-Erk-2 monomer adducts are formed when Erk-2 is exposed to this range of 4-HNE concentrations. This blot shows that a stable 41-kDa adduct is formed after exposure to 1 to 100 μM 4-HNE (5:1, 50:1, and 500:1 M ratios, respectively, 4-HNE:Erk-2). At the highest concentration evaluated (100 μM 4-HNE), adduct formation results in cross-linked Erk-2 monomers as indicated by a minor band shift from 41 kDa to 82 and 123 kDa at 100 μM 4-HNE. Concurrent with the formation of the cross-linked 4-HNE-Erk-2 adducts, identical blots probed for total Erk-1/2 (Fig. 5B) show a marked decrease of the positive signal at 100 μM 4-HNE. These data show that the major 4-HNE adduct formed with Erk-2 is the monomer, which is consistent with observations using extracts from hepatocytes exposed to 4-HNE (Fig. 3C) or iron (Fig. 3D).

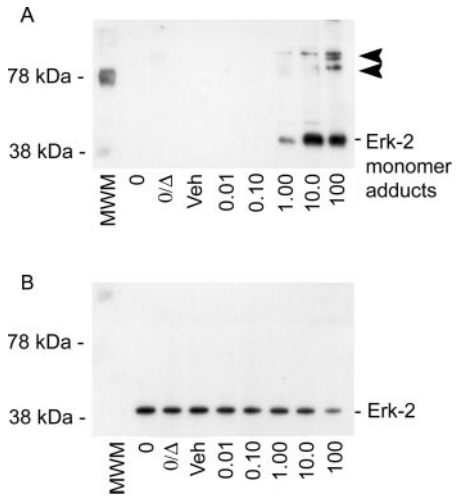

Fig. 5. 4-HNE was tested for its ability to form covalent adducts with inactive Erk-2 in vitro, over a range of molar ratios of aldehyde to protein associated with escalating oxidative stress in vivo. A, representative immunoblot demonstrating Erk-2 exposure to increasing 4-HNE concentrations increased aldehyde-modified Erk-2 monomers from 1.0 to 100.0 μM. At the highest concentration 4-HNE caused the covalent cross-linking of Erk-2 monomers, as indicated by the arrows to the right of the image. B, representative immunoblot analysis of the blot in A stripped and reprobed for total Erk-1/2, showing no change in Erk-2 levels until the progressive loss observed from 1.0 to 100.0 μM, suggesting covalent cross-linking of proteins masks the epitope for antibody recognition. (MWM, molecular weight marker; 0, no treatment; 0/Δ, no treatment with heat; Veh, vehicle control; 0.01–100, micromolar concentration of 4-HNE).

LC-MS/MS Analysis of 4-HNE-Erk-2 Monomer Adducts Reveals Modification at His 178. The data presented in Figs. 2 to 5 suggest the presence of specific nucleophilic residues in Erk-1/2, which, when modified by 4-HNE, result in decreased phosphorylation and activity. To identify these nucleophilic residues, in vitro modification of Erk-2 by 4-HNE was carried out as described above, and concentrations of 0, 10, and 100 μM 4-HNE were used, representing aldehyde to protein molar ratios of 0:1, 50:1, and 500:1, respectively (4-HNE:Erk-2). Tryptic peptides from control and treated Erk-2 were evaluated by LC-MS/MS to determine the specific location(s) of 4-HNE modification(s). The total ion chromatograms (Fig. 6, A–F) show that Erk-2 incubated with 10 or 100 μM 4-HNE (medium and large arrows, respectively) resulted in a loss of signal intensity for the peptides eluting at 15.6, 16.2, and 20.6 min (Fig. 6, A, C, and E, respectively) compared with the 0 μM 4-HNE control (small arrows). Further analysis of these data demonstrate increasing signal intensity for peaks eluting at 17.2, 24.2, and 21.7 min (Fig. 6, B, D, and F, respectively) that correlated with increasing concentrations of 4-HNE treatment, as indicated by the increasing arrow sizes. It is important to note that the peaks increasing in intensity shown in Fig. 6, B, D, and F elute at greater retention times (i.e., 1.1–8.0 min) using a C18 column representing peptides more hydrophobic than those in Fig. 6, A, C, and E, which would indicate the presence of a lipid adduct such as 4-HNE.

Analysis of these peptides via mass spectrometry (MS) revealed the mass/charge ratio (m/z) for the peaks shown in Fig. 6, A, C, and E to be at 2143.0, 1508.7, and 3160.2, respectively, as shown in Fig. 7, A, C, and E. In addition, MS analysis of the peaks shown in Fig. 6, B, D, and F correspond to m/z values at 2299.1, 1665.3, and 3543.9, respectively, as shown in Fig. 7, B, D, and F. Based on mass calculated using the MS-digest feature of Protein Prospector, the peaks at m/z 2143.0, 1508.8, and 3160.2 correspond to peptides derived from protein residues 171–189, 54–65, and 230–257, respectively, and the peaks at m/z 2299.0, 1665.3, and 3543.9 resulting from peptides of protein residues 171–189, 54–65, and 230–259 plus a 4-HNE molecule (156 Da). MS/MS analysis confirmed the sequences and identified the specific residues adducted within peptides 171 to 189 and 230 to 259 as His 178 and His 230 as indicated in the peptide sequences of Table 1 and the three-dimensional images in Fig. 8, A and C, respectively. The triply charged peak (at m/z 767.66) of the 19-residue peptide (aa 171–189) containing the 4-HNE adduct was subjected to fragmentation, yielding major ions

consistent with an adduct on His 178 (Fig. 7 legend). Likewise, the triply charged peak (at m/z 1181.75) of the 4-HNE-adducted 30-residue peptide (aa 230–259) was fragmented yielding major ions consistent with an adduct on His 230 (Fig. 7 legend). The inability of tandem MS to confirm the specific location of the adduct within the MS-identified peptide at 1665.3 m/z, is probably associated with the lower stability of 4-HNE-Cys adducts, compared with 4-HNE-His adducts. Therefore, the 4-HNE-adducted peptide 54–65 was confirmed based on the original mass spectra indicating the +1, +2, and +3 ions with m/z values of 1665.3, 833.2, and 555.8, respectively. These data are summarized in Table 1. It is important to note that only the His 178 adduct within the phosphorylation lip was identified using both the 10 and 100 μM treatment groups, whereas the Cys 63 and His 230 adducts were detected using only the 100 μM concentration of 4-HNE. Cys 63 lies within the α-helix of the N-terminal domain, and His 230 maps to an α-helix within the C-terminal domain, which could also explain the concentration differences between the formation of these two adducts and the His 178 adducts within the phosphorylation loop. However, all three adduct sites are solvent accessible and are within or are in proximity to the active site at the domain interface (Fig. 8).

Discussion

It is well established that the autocatalytic degradation of membrane lipids accompanying oxidative stress results in the production of reactive α/β-unsaturated lipid aldehydes (Esterbauer et al., 1991; Ishii, 1996). Recent evidence demonstrates that chronic exposure to the pro-oxidant ethanol results in the loss of constitutive Erk-1/2 phosphorylation in vivo and in primary culture (Hendrickson et al., 1998; Aroor and Shukla, 2004; Chandler and Sutton, 2005). However, the connection between pro-oxidant-induced lipid peroxidation and the inhibition of the Erk-1/2 signal transduction pathway is unknown. In this study, we investigated the possibility that the lipid peroxidation product 4-HNE may mediate pro-oxidant-induced loss of hepatic Erk-1/2 activity using primary hepatocyte cultures. We also investigated the mechanism of aldehyde-mediated inhibition of kinase signaling by analyzing 4-HNE-modified amino acid residues that occur within the inactive Erk. These results show that subtoxic concentrations of 4-HNE as well as a pro-oxidant challenge using iron ascorbate, an iron chelate previously shown to cause lipid peroxidation and 4-HNE-protein adduct formation in primary hepatocyte cultures (Hartley et al., 1997), inhibit Erk-1/2 signaling.

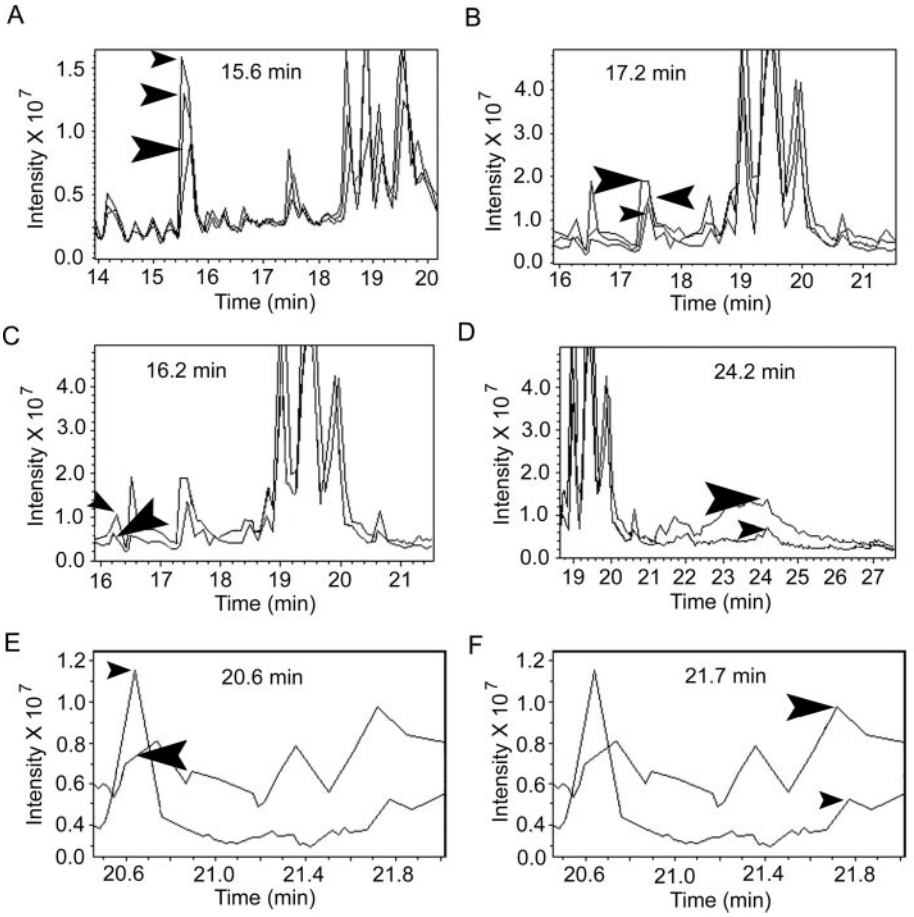

Fig. 6. LC was used to characterize the effects of 4-HNE on inactive Erk-2 in vitro by using tryptic peptides of native and aldehyde-modified protein. A, compared with untreated Erk-2 (small arrow), the parent peak at 15.6 min decreased with 10 and 100 μM 4-HNE treatment (medium and large arrows, respectively), which corresponded to an increase in the peak eluting at 17.2 min from 0.0 to 10.0 to 100.0 μM 4-HNE (small, medium, and large arrows, respectively) (B). Similar to A, C and E demonstrate a loss of parent peaks at 16.2 and 20.6 min, respectively, which also associated with an associated increase in peaks eluting at 24.2 and 21.7 min, respectively (D and F). Unlike the peaks identified in A and B, the peaks in C to F only changed with 100 μM 4-HNE treatment.

The identification of 4-HNE as the most abundant and reactive aldehydic by-product of lipid peroxidation (Benedetti et al., 1980; Esterbauer et al., 1991) has resulted in intense research focused on this bioactive molecule as a mediator of the pathological mechanisms of chronic diseases associated by oxidative stress. Past evidence based on model systems using immortalized cell lines suggested that 4-HNE is capable of mediating the activation of Erk-1/2 in vitro (Iles et al., 2003; Iles and Liu, 2005). It has been suggested by others that these observations result from the direct interaction of 4-HNE with the EGF-receptor to initiate the kinase cascade that would produce this outcome (Liu et al., 1999), although the activation of this proliferative pathway was associated with growth inhibition in this latter study. In the present study, we demonstrate that 4-HNE inhibits constitutive Erk-1/2 phosphorylation and activity by forming covalent adducts with inactive Erk monomers. Specifically, using primary rat hepatocytes as a cellular model, we observed that physiologically relevant levels of 4-HNE inhibited Erk-1/2 phosphorylation (Fig. 2C), activity (Fig. 3A) as well as nuclear localization (Fig. 4A). In addition, 4-HNE treatment of primary hepatocytes resulted in the concentration-dependent loss of Elk-1 and AP-1 phosphorylation (Fig. 4, C and D, respectively), and the suppression of nuclear cFos and cJun activity toward the TRE sequence (Fig. 4, E and F, respectively), with 100 μM 4-HNE resulting in the complete ablation of cFos

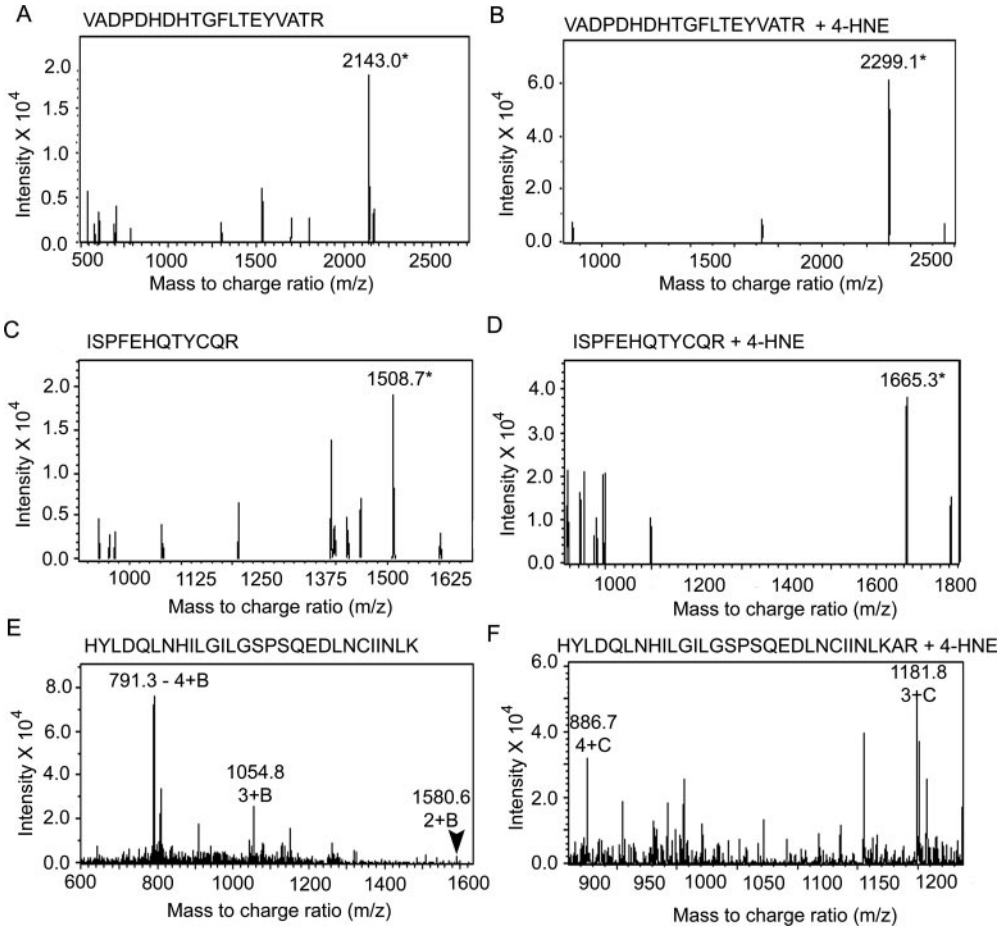

Fig. 7. Mass spectral (MS) analysis was used to identify the changing peaks identified by LC in Fig. 6, and MS/MS was used to confirm the corresponding peptide sequences and specific amino acid target of protein adduction. A, deconvoluted spectrum of the peptide eluting at 15.6 min (Fig. 6A) showing a parent ion peak at 2143.0 m/z, corresponding to amino acid sequence VADPDHDHTGFLTEYVATR of Erk-2 (aa 171–189), which was confirmed by MS/MS. B, mass spectra of the peptide eluting at 17.2 min (Fig. 6B) showing a parent ion peak at 2299.1 m/z, corresponding to amino acid sequence VADPDHDHTGFLTEYVATR + (1) 4-HNE molecule (156 Da). The amino acid location of the adduct was identified by MS/MS fragmentation analysis of the triply charged peak (at m/z 767.66) of the 19-residue peptide (aa 171–189) containing the 4-HNE adduct, yielding the following major ions, consistent with an adduct on His 178: $b^{++}{}_{11}$ (674.81), $b^{++}{}_{12}$ (731.35), $b^{0++}{}_{12}$ (722.35), $b^{++}{}_{13}$ (781.88), $b^{0++}{}_{13}$ (772.87), $b^{++}{}_{14}$ (846.4), $b^{0++}{}_{14}$ (837.39), $b^{++}{}_{15}$ (927.93), $b^{++}{}_{18}$ (1063.51), y_5 (609.34), $y^*{}_5$ (592.31), y_6 (738.38), y_7 (839.43), y_8 (952.51), $y^*{}_8$ (935.48), y_{10} (1156.60), **y_{11} (1257.65), $y^{++}{}_{12}$ (775.91)**, $y^{*++}{}_{12}$ (767.40), $y^{0++}{}_{12}$ (766.91), $y^{0++}{}_{13}$ (824.42), $y^{++}{}_{16}$ (1008.00). C, deconvoluted spectra of the LC peak eluting at 16.2 min (Fig. 6C) showing a parent ion peak of 1508.7 m/z, which corresponds to the amino acid sequence ISPFEHQTYCQR of Erk-2 (aa 54–65). This sequence was confirmed by MS/MS. D, deconvoluted spectrum of the peptide eluting at 24.2 min (Fig. 6D) showing a parent ion peak at 1665.3 m/z, corresponding to amino acid sequence ISPFEHQTYCQR + (1) 4-HNE. MS/MS analysis of this peptide confirmed the sequence, however, was unable to confirm the specific location of the 4-HNE adduct, suggesting an unstable cysteine adduct at Cys 63. E, mass spectral analysis of the peptide eluting at 20.6 min (Fig. 6E) showing +2, +3, and +4 ion peaks corresponding to the amino acid sequence HYLDQLNHILGILGSPSQEDLNCIINLK of Erk-2 (aa 230–259). This sequence was confirmed by MS/MS fragmentation analysis. F, mass spectral analysis of the peptide eluting at 21.7 min (Fig. 6F) showing the +3 and +4 ion peaks corresponding to the amino acid sequence HYLDQLNHILGILGSPSQEDLNCIINLKAR + (1) 4-HNE molecule. MS/MS fragmentation analysis of the triply charged peak (at m/z 1181.75) of the 4-HNE-adducted 30-residue peptide (aa 230–259) yielded major ions consistent with an adduct on His 230: **b_5 (813.41), b_{10} (1403.77)**, $b^{++}{}_{17}$ (1008.05), $b^{++}{}_{18}$ (1072.08), $b^{++}{}_{21}$ (1250.66), $b^{++}{}_{26}$ (1529.29), y_{10} (1157.68), $y^{0++}{}_{11}$ (627.85), y_{13} (1529.81), y_{17} (1857.95), **$y^{*++}{}_{21}$ (1119.10), y_{23} (2504.37),** $y^{*++}{}_{23}$ (1244.17), $y^{0++}{}_{23}$ (1243.68). Bold indicates ions crucial for identifying the specific amino acid location of the adduct.

activity. These results were supported by data showing that the iron-induced lipid peroxidation caused a similar concentration-dependent decrease in Erk-1/2 phosphorylation (Fig. 2C) and activity (Fig. 3B). It is noteworthy that 4-HNE treatment of active, phosphorylated Erk-1/2 had no effect on Erk-1/2 activity (Fig. 3A, inset), indicating that, using our experimental model, inhibition of kinase activity by 4-HNE occurs through aldehyde interactions with the inactive Erk monomers. Data showing that both 4-HNE- and iron-induced inhibition of Erk-1/2 correlates with increasing concentrations of 4-HNE-Erk-1/2 monomer adducts (Fig. 3, C and D, respectively) further support this hypothesis. Together, these data indicate that 4-HNE inhibits Erk-Elk-AP-1 signal transduction in hepatocytes, possibly by forming covalent adducts with the inactive Erk monomers.

The mechanism of 4-HNE inhibition of enzymatic activity has been proposed whereby covalent modification of nucleophilic residues within the proteins, which are crucial to proper enzymatic function, result in the loss of activity (Ji et al., 2001; Carbone et al., 2004a, 2005a,b). Studies investigating the effects of chronic ethanol-induced oxidative stress on normal liver function have recently shown that 4-HNE modification of liver enzymes such as heat shock protein 72, heat shock protein 90, and protein disulfide isomerase inhibits enzyme activity resulting from the irreversible modification of functionally important amino acids (Carbone et al., 2004a, 2005a,b). Using immunoblot analysis, in the present study, we showed that 4-HNE covalently modifies inactive Erk-2 monomers at molar ratios consistent with increasing oxidative stress (Fig. 5A). Analysis of tryptic peptides from native and 4-HNE-modified Erk-2 was carried out using LC-MS/MS. LC analysis identifies the loss of parent peptides with 4-HNE treatment (Fig. 6, A, C, and D) that correlates with an increase in more hydrophobic peaks eluting at later times (Fig. 6, B, D, and F), an observation consistent with the addition of the nine-carbon 4-HNE molecule. MS/MS analysis of the major 4-HNE-Erk-2 monomer adduct shown in Fig. 5 identifies the location of this adduct to be at His 178 within the phosphorylation lip of the Erk-2 monomer (Figs. 7B and 8A). His 178 lies within a few residues of the Tyr/Thr phosphorylation sites of the Erk-2 activation loop and is a crucial residue in the shift from the inactive to active conformation of both Erk-1 and Erk-2 (Cobb et al., 1994; Chen et al., 2001), implicating stearic and/or conformational hindrance of phosphorylation from upstream kinases by the addition of a nine carbon molecule at this location. Whereas additional investigations will be necessary to confirm the amino acid residues of Erk-1/2 that are critical targets for modification by 4-HNE, these findings provide new insight into the molecular mechanisms by which 4-HNE modulates Erk-1/2 signal transduction and potentially gene expression in hepatocytes.

The loss of Erk-mediated gene expression has vast physiological implications with respect to hepatocellular survival in the context of chronic, repeated toxic insult. Inhibition of Erk-Elk-AP-1 signaling suggests the ability of 4-HNE to suppress the Erk-mediated proliferation, survival, and homeostasis in hepatocytes, and it may reveal a sensitizing event in chronic diseases associated with oxidative stress. Other research demonstrates that inhibition of Erk results in cell sensitization to toxic insult (Jazirehi et al., 2004), a situation important to chronic hepatic disease states related by oxidative stress, such as alcoholic liver disease, chronic iron overload, hepatitis C, and primary biliary cirrhosis (Paradis et al., 1997a,b). In addition, it has been shown that chronic ethanol exposure suppresses the ability of the liver to regenerate after partial hepatectomy or toxic injury (Wands et al., 1979; Duguay et al., 1982), although a mechanism of inhibition is not known. Impairment of the Erk-1/2 signaling pathway can potentially suppress hepatocellular proliferation via the loss of cFos transcription factor activity, as shown in cells treated with pathologically relevant concentrations of 4-HNE (Fig. 4E). In addition, the suppression of the pro-apoptotic cJun transcription factor could potentially result in the accumulation of old dysfunctional cells that would otherwise be removed via programmed cell death. Although the observed loss of cJun activity as a result of 4-HNE exposure contradicts previous studies showing 4-HNE activation of AP-1 through the adduction and activation of SAPK/JNK (Parola et al., 1998), these previous studies incorporated nonparenchymal cells, which are probably disparate from the parenchymal cells observed in the studies reported herein with respect to basal proliferative activity and 4-HNE metabolic capacity, and therefore sensitivity. In addition, Parola et al. (1998) also showed no effect of 4-HNE on Ras/Erk activity, cFos expression, or nuclear factor-κB activity, the latter of which was shown to be directly inhibited by 4-HNE in other studies (Ji et al., 2001). The hypothesis that 4-HNE inhibition of Erk-1/2 is a sensitizing event

TABLE 1

LC/MS/MS analysis of the tryptic peptides of recombinant Erk-2 reacted with 4-HNE

Summary of data shown in Figs. 6, 7, and 8. Amino acid positions of the identified adducts are shown in bold within the peptide sequence and described by their amino acid position within the full-length peptide.

Position[a]	Peptide[b]	RT (min)	$[MH]^+$ calculated	$[MH]^+$ observed	Adduct	[4-HNE][c]
						μM
171–189	VADPDHDHTGFLTEYVATR	15.6	2144.0	2143.0	None	0, 10, 100
171–189	VAPDPHD**H**TGFLTEYVATR + 4HNE	17.2	2300.1	2299.1	His 178	10*,[d]100
54–65	ISPFEHQTYCQR	16.2	1508.7	1508.7	None	0, 10, 100
54–65	ISPFEHQTYCQR + 4HNE	24.2	1664.8	1665.3	Cys 63	100
230–257	HYLDQLNHILGILGSPSWEDLNCIINLK	20.6	3160.6	3160.2	None	0, 10, 100
230–259	**H**YLDWLNHILGILGSPSWEDLNCIINLKAR + 4HNE	21.7	3543.9	3543.9	His 230	100

[a] Position of residues in protein.
[b] Peptide sequence. Note that modified residue is in bold and larger font.
[c] Treatment with 4-HNE at specified concentrations yielding peak observed.
[d] 10* indicates treatment conditions associated with monomer adducts identified in primary culture studies. Asterisk denotes aldehyde concentration associated with Erk monomer adduct.

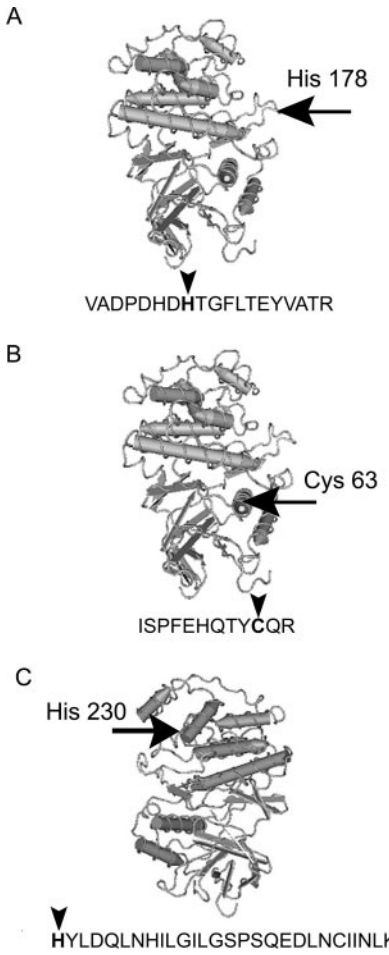

Fig. 8. Locations of the three 4-HNE adducts on Erk-2 identified by LC-MS/MS analysis A, His 178 adduct within the phosphorylation lip of Erk-2 identified after treatment of protein with both 10 and 100 μM 4-HNE and corresponding to Figs. 6B and 7B. B, Cys 63 adduct within the α-helix C of Erk-2 was identified after 100 μM 4-HNE treatment only and corresponding to Figs. 6D and 7D. C, His 230 adduct within an α-helix of the domain interface of Erk-2 was identified after 100 μM 4-HNE treatment only and corresponding to Figs. 6F and 7F. All three adducts were found to occur at solvent accessible locations within the three dimensional structure of Erk-2.

associated with the oxidative stress that accompanies many diseases is consistent with research showing that lipid peroxidation and the accumulation of 4-HNE-protein adducts are early events in the evolution of chronic alcoholic liver disease (Sampey et al., 2003; Ronis et al., 2005).

In summary, the data presented here reveal that 4-HNE inhibits Erk-1/2 phosphorylation and activity via aldehyde-protein adduct formation with the inactive Erk monomers. In primary rat hepatocytes, 4-HNE inhibition of Erk-1/2 results in the loss of signal transduction through Elk-1 and the AP-1 constituents cFos and cJun. Modification of His 178 within the phosphorylation loop of Erk-2, a residue conserved within the redundant Erk-1 molecule, identifies a novel mechanism whereby 4-HNE inhibits signal transduction, which potentially affects hepatocyte proliferation, survival, and homeostasis through the loss of normal AP-1 transcription factor activity.

References

Aroor AR and Shukla SD (2004) MAP kinase signaling in diverse effects of ethanol. *Life Sci* **74:**2339–2364.

Bae MA, Soh Y, Pie JE, and Song BJ (2000) Selective activation or the C-Jun N-terminal protein kinase pathway during acetaminophen-induced apoptosis. *FASEB J* **14:**A1516.

Benedetti A, Casini AF, Ferrali F, and Comporti M (1979) Effects of diffusible products of lipid peroxidation on liver microsomal lipids. *Biochem J* **180:**303–312.

Benedetti A, Comporti M, and Esterbauer H (1980) Identification of 4-Hydroxynoneal as a cyto-toxic product originating from the peroxidation of liver microsomal lipids. *Biochim Biophys Acta* **620:**281–296.

Canuto RA, Ferro M, Muzio G, Bassi AM, Leonarduzzi G, Maggiora M, Adamo D, Poli G, and Lindahl R (1994) Role of aldehyde metabolizing enzymes in mediating effects of aldehyde products of lipid-peroxidation in liver-cells. *Carcinogenesis* **15:**1359–1364.

Canuto RA, Muzio G, Maggiora M, Poli G, Biasi F, Dianzani MU, Ferro M, Bassi AM, Penco S, and Marinari UM (1993) Ability of different hepatoma-cells to metabolize 4-hydroxynonenal. *Cell Biochem Funct* **11:**79–86.

Carbone DL, Doorn JA, Kiebler Z, Ickes BR, and Petersen DR (2005a) Modification of heat shock protein 90 by 4-hydroxynonenal in a rat model of chronic alcoholic liver disease. *J Pharmacol Exp Ther* **315:**8–15.

Carbone DL, Doorn JA, Kiebler Z, and Petersen DR (2005b) Cysteine modification by lipid peroxidation products inhibits protein disulfide isomerase. *Chem Res Toxicol* **18:**1324–1331.

Carbone DL, Doorn JA, Kiebler Z, Sampey BP, and Petersen DR (2004a) Inhibition of Hsp72-mediated protein refolding by 4-hydroxy-2-nonenal. *Chem Res Toxicol* **17:**1459–1467.

Carbone DL, Doorn JA, and Petersen DR (2004b) 4-Hydroxynonenal regulates 26S proteasomal degradation of alcohol dehydrogenase. *Free Radic Biol Med* **37:**1430–1439.

Chandler LJ and Sutton G (2005) Acute ethanol inhibits extracellular signal-regulated kinase, protein kinase B, and adenosine 3′:5′-cyclic monophosphate response element binding protein activity in an age- and brain region-specific manner. *Alcohol Clin Exp Res* **29:**672–682.

Chen JP, Ishac EJN, Dent P, Kunos G, and Gao B (1998) Effects of ethanol on mitogen-activated protein kinase and stress-activated protein kinase cascades in normal and regenerating liver. *Biochem J* **334:**669–676.

Chen Z, Gibson TB, Robinson F, Silvestro L, Pearson G, Xu BE, Wright A, Vanderbilt C, and Cobb MH (2001) MAP kinases. *Chem Rev* **101:**2449–2476.

Cobb MH, Hepler JE, Cheng MG, and Robbins D (1994) The mitogen-activated protein-kinases, Erk1 and Erk2. *Semin Cancer Biol* **5:**261–268.

Davis MI, Szarowski D, Turner JN, Morrisett RA, and Shain W (1999) In Vivo Activation and in situ BDNF-stimulated nuclear translocation of mitogen-activated/extracellular signal-regulated protein kinase is inhibited by ethanol in the developing rat hippocampus. *Neurosci Lett* **272:**95–98.

Doorn JA and Petersen DR (2002) Covalent modification of amino acid nucleophiles by the lipid peroxidation products 4-hydroxy-2-nonenal and 4-oxo-2-nonenal. *Chem Res Toxicol* **15:**1445–1450.

Duguay L, Coutu D, Hetu C, and Joly JG (1982) Inhibition of liver-regeneration by chronic alcohol administration. *Gut* **23:**8–13.

Esterbauer H, Schaur RJ, and Zollner H (1991) Chemistry and biochemistry of 4-hydroxynonenal, malonaldehyde and related aldehydes. *Free Radic Biol Med* **11:**81–128.

Hartley DP, Kroll DJ, and Petersen DR (1997) Pro-oxidant-initiated lipid peroxidation in isolated rat hepatocytes: detection of 4-hydroxynonenal- and malondialdehyde-protein adducts. *Chem Res Toxicol* **10:**895–905.

Hartley DP and Petersen DR (1997) Co-metabolism of ethanol, ethanol-derived acetaldehyde, and 4-hydroxynonenal in isolated rat hepatocytes. *Alcohol Clin Exp Res* **21:**298–304.

Hendrickson RJ, Cahill PA, McKillop IH, Sitzmann JV, and Redmond EM (1998) Ethanol inhibits mitogen activated protein kinase activity and growth of vascular smooth muscle cells in vitro. *Eur J Pharmacol* **362:**251–259.

Iles KE, Dickinson DA, Wigley AF, Welty NE, and Forman HJ (2003) HNE induces HO-1 through activation of the ERK and JNK pathways in alveolar type II cells. *Free Radic Biol Med* **35:**S67.

Iles KE and Liu RM (2005) Mechanisms of glutamate cysteine ligase (GCL) induction by 4-hydroxynonenal. *Free Radic Biol Med* **38:**547–556.

Ishii H (1996) Oxidative stress in alcoholic liver injury. *Alcohol Clin Exp Res* **20:**162A–167A.

Jazirehi AR, Vega MI, Chatterjee D, Goodglick L, and Bonavida B (2004) Inhibition of the Raf-MEK1/2-ERK1/2 signaling pathway, Bcl-(XL) down-regulation, and chemosensitization of non-Hodgkin's lymphoma B cells by rituximab. *Cancer Res* **64:**7117–7126.

Ji C, Kozak KR, and Marnett LJ (2001) IκB kinase, a molecular target for inhibition by 4-hydroxy-2-nonenal. *J Biol Chem* **276:**18223–18228.

Karin M (1995) The regulation of AP-1 activity by mitogen-activated protein-kinases. *J Biol Chem* **270:**16483–16486.

Liu W, Akhand AA, Kato M, Yokoyama I, Miyata T, Kurokawa K, Uchida K, and Nakashima I (1999) 4-Hydroxynonenal triggers an epidermal growth factor receptor-linked signal pathway for growth inhibition. *J Cell Sci* **112:**2409–2417.

Mitchell DY and Petersen DR (1991) Inhibition of rat hepatic mitochondrial aldehyde dehydrogenase mediated acetaldehyde oxidation by trans-4-hydroxy-2-nonenal. *Hepatology* **13:**728–734.

Paradis V, Kollinger M, Fabre M, Holstege A, Poynard T, and Bedossa P (1997a) In situ detection of lipid peroxidation by-products in chronic liver diseases. *Hepatology* **26:**135–142.

Paradis V, Mathurin P, Kollinger M, ImbertBismut F, Charlotte F, Piton A, Opolon P, Holstege A, Poynard T, and Bedossa P (1997b) In situ detection of lipid peroxidation in chronic hepatitis c: correlation with pathological features. *J Clin Pathol* **50:**401–406.

Parola M, Robino G, Marra F, Pinzani M, Bellomo G, Leonarduzzi G, Chiarugi P,

Camandola S, Poli G, Waeg G, et al. (1998) HNE interacts directly with JNK isoforms in human hepatic stellate cells. *J Clin Investig* **102:**1942–1950.
Pearson G, Robinson F, Gibson TB, Xu BE, Karandikar M, Berman K, and Cobb MH (2001) Mitogen-activated protein (MAP) kinase pathways: regulation and physiological functions. *Endocr Rev* **22:**153–183.
Ronis MJJ, Butura A, Sampey BP, Shankar K, Prior RL, Korourian S, Albano E, Ingelman-Sundberg M, Petersen DR, and Badger TM (2005) Effects of N-acetylcysteine on ethanol-induced hepatotoxicity in rats fed via total enteral nutrition. *Free Radic Biol Med* **39:**619–630.
Sampey BP, Korourian S, Ronis MJ, Badger TM, and Petersen DR (2003) Immunohistochemical characterization of hepatic malondialdehyde and 4-hydroxynonenal modified proteins during early stages of ethanol-induced liver injury. *Alcohol Clin Exp Res* **27:**1015–1022.
Schaur RJ, Zollner H, and Esterbauer H (1990) Biological effects of aldehydes with particular attention to 4-hydroxynonenal and malondialdehyde, in *Membrane Lipid Peroxidation*, pp 141–163, CRC Press, Boca Raton, FL.
Tjalkens RB, Luckey SW, Kroll DJ, and Petersen DR (1998) alpha, beta-Unsaturated aldehydes increase glutathione S-transferase MRNA and protein: correlation with activation of the antioxidant response element. *Arch Biochem Biophys* **359:**42–50.
Tyagi A, Agarwal R, and Agarwal C (2003) Grape seed extract inhibits EGF-induced and constitutively active mitogenic signaling but activates JNK in human prostate carcinoma DU145 cells: possible role in antiproliferation and apoptosis. *Oncogene* **22:**1302–1316.
Wands JR, Carter EA, Bucher NLR, and Isselbacher KJ (1979) Inhibition of hepatic regeneration in rats by acute and chronic ethanol intoxication. *Gastroenterology* **77:**528–531.
Watanabe T, Pakala R, Katagiri T, and Benedict CR (2001) Lipid peroxidation product 4-hydroxy-2-nonenal acts synergistically with serotonin in inducing vascular smooth muscle cell proliferation. *Atherosclerosis* **155:**37–44.

Address correspondence to: Dr. Dennis R. Petersen, University of Colorado Health Sciences Center, School of Pharmacy, 4200 East Ninth Ave., Box C238, Denver, CO 80262. E-mail: dennis.petersen@uchsc.edu